Chin. J. Astron. Astrophys. Vol. 4 (2004), No. 2, 143–152
(http://www.chjaa.org or http://chjaa.bao.ac.cn)

Chinese Journal of Astronomy and Astrophysics

Evolution of M81 with Exponentially Decreasing Star Formation Rate of PEGASE *

Jiu-Li Li, Xu Zhou, Jun Ma and Jian-Sheng Chen

National Astronomical Observatories, Chinese Academy of Sciences, Beijing 100012;
ljl@vega.bac.pku.edu.cn

Received 2003 July 29; accepted 2004 March 2

Abstract Based on the large field multicolor observations of Beijing-Arizona-Taiwan-Connecticut (BATC) program, we obtain the spectral energy distribution (SED) for individual regions of M81. We study the structure and evolution of M81 with an evolutionary population synthesis (EPS) model, PEGASE. We find that the exponentially deceasing star formation rate (SFR) with star formation scale 3 Gyr (hereafter Exp, $\tau = 3$ Gyr) gives the best agreement between the model predictions and the observed SEDs. We then obtain the structure, age distribution and evolutionary history of M81. There is a clear age gradient between the central and outer regions. The populations in the central regions are older than 7 Gyr, those in the outer regions are younger, at about 4.5 Gyr. The youngest components in the spiral arms have ages of about 2.5 Gyr or less.

Key words: galaxies: individual (M81) – galaxies: evolution – galaxies: star general

1 INTRODUCTION

M81 is a beautiful nearby early-type Sab spiral galaxy, at a distance of 3.6 Mpc and with an angular size of $\sim 26'$ (Freedman et al. 1994). The galaxy is interesting and important because: (1) it is the nearest example of a galaxy that exhibits both LINER (Heckman et al. 1980) and Seyfert 1 (Peimbert & Torres-Peimbert 1981) characteristics; (2) there is a filamentary emission-line spiral residing inside its bulge (Jacoby et al. 1989). It has been the subject of numerous studies on galactic structure.

Our collaborative effort, the BATC Multicolor Sky Survey (Fan et al. 1996; Zheng et al. 1999; Zhou et al. 2001), has already observed this spiral galaxy as part of its galaxy calibration program. The BATC program uses the 60/90 cm Schmidt telescope at the Xinglong Station of National Astronomical Observatories of China (NAOC), with its focal plane equipped with a 2048×2048 Ford CCD and a set of 15 intermediate-band filters that was designed to obtain spectrophotometry for pre-selected 1 deg^2 regions of the northern sky.

* Supported by the National Natural Science Foundation of China.

EPS is a technique to model the spectrophotometric properties of stellar populations, based on our knowledge of stellar evolution. Since the fundamental work of Tinsley (1972) and Searle, Sargent & Bagnuolo (1973), EPS has become a standard technique to study the stellar populations of galaxies. As the simplest EPS model, SSP (simple stellar population) can be applied to the study of stellar population such as star clusters. The SSP is defined as a single generation of coeval stars with fixed parameters, such as metallicity, age and initial mass function (IMF), etc. (Buzzoni 1999). The concept of SSP is important because complex stellar systems can be modelled by convolving SSPs with the adopted star formation history. PEGASE (Fioc & Rocca-Volmerange 1997) is a widely used EPS model for describing the evolution of galaxies. It has been used to describe instantaneous starburst, or constant or exponentially decreasing (or increasing) star formation. Using this model, the physical properties of the galaxy can be derived from its continuous spectrum. In PEGASE, the stellar initial mass function, the star formation rate (SFR), and stellar atmosphere formulations are all adjustable initial parameters (Kewley 2001). Besides the EPS models, other well-known models include GISSEL96 (Charlot & Bruzual 1991; Bruzual & Charlot 1993; Bruzual & Charlot 1996), STARBURST99 (Leitherer et al. 1999), etc.

As we know, multicolor photometry is able to provide accurate SEDs for the whole galaxy. As the first work of our series on galactic structure, Kong et al. (2000) presented the observation and data reduction of M81, and gave the distributions of age, metallicity and reddening with the SSPs of GISSEL96 (GSSPs). In this paper, we continue our study on the structure and the evolution of M81 with PEGASE on the basis of Kong et al. (2000). Different from GSSPs, PEGASE affords an evolutionary spectral synthesis and can give the evolutionary history of the galaxy. By comparing in detail the fitting results from three forms of SFR in PEGASE, we find the exponential form of star formation (ESF) is the most satisfactory for describing the evolution of M81. From the comparison of fitting results and further analysis with GSSPs and PEGASE, it is shown that ESF of PEGASE is appropriate to outline the evolution of the galaxy.

The present paper is structured as follows. Observations and data reduction are described in Section 2. In Section 3, we provide a brief description of PEGASE and the fitting algorithm. The structure and age distribution of M81 are described in Section 4 and a discussion is given in Section 5. Our main conclusions are summarized in Section 6.

2 OBSERVATIONS AND DATA REDUCTION

Large-field, multicolor images of the spiral galaxy M81 were obtained on the BATC photometric system. A full description of the NAOC Schmidt Telescope, CCD camera, data-acquisition system and definition of BATC filter system can be found in Fan et al. (1996) and Zhou et al. (2003). The data were reduced with the automatic data reduction software named PIPELINE I developed for BATC multicolor sky survey (Fan et al. 1996). Standard procedures including bias subtraction, dark subtraction, flat-fielding, sky background fitting and flux calibration were performed. Detailed procedure of image data reduction can be seen in Kong et al. (2000). Thus, we can acquire two-dimensional SED map of M81. The ADU value of each image was converted into units of 10^{-30} erg s^{-1} cm^{-2} Hz^{-1}. As an example, we present in Table 1 the SED of some of the areas of M81. Columns (1) and (2) show the (X,Y) positions (in units of pixel) of the photometric center of the area; columns (3)–(15) present the flux in 13 filters in units of 10^{-30} erg s^{-1} cm^{-2} Hz^{-1}. The uncertainties in the fluxes are given in the next line.

Table 1 The SED in Different Areas of M81 (10^{-30} erg s^{-1} cm^{-2} Hz^{-1})

X	Y	02	04	05	06	07	08	09	10	11	12	13	14	15
(1)	(2)	(3)	(4)	(5)	(6)	(7)	(8)	(9)	(10)	(11)	(12)	(13)	(14)	(15)
361	401	48.4	128.1	136.5	167.0	243.0	261.7	312.7	359.3	369.2	427.6	433.4	542.1	565.5
		3.6	5.9	3.2	3.9	5.5	6.4	3.7	8.6	5.8	7.7	9.1	11.7	12.3
361	402	47.3	126.0	133.6	164.6	239.0	258.5	306.9	353.4	362.1	420.9	426.3	529.9	555.9
		3.6	5.9	3.1	3.9	5.4	6.4	3.7	8.6	5.8	7.7	9.1	11.6	12.3
361	403	47.0	124.2	132.1	161.9	235.5	256.0	304.4	351.5	357.9	417.5	426.5	525.2	550.7
		3.6	5.9	3.1	3.8	5.4	6.4	3.7	8.6	5.7	7.6	9.1	11.5	12.2
361	404	47.0	122.1	129.9	159.1	231.8	253.1	300.5	348.5	352.8	412.6	423.6	518.3	544.7
		3.6	5.8	3.1	3.8	5.4	6.4	3.7	8.5	5.7	7.6	9.1	11.5	12.1
361	405	46.5	121.4	128.5	157.0	228.4	248.9	295.7	344.6	347.4	406.2	414.7	509.3	536.8
		3.5	5.8	3.1	3.8	5.4	6.3	3.7	8.5	5.7	7.6	9.0	11.4	12.1
361	406	45.6	117.6	125.6	152.4	223.8	245.3	291.3	340.7	342.1	399.2	412.7	500.8	526.9
		3.5	5.8	3.1	3.8	5.3	6.3	3.6	8.5	5.6	7.5	9.0	11.3	12.0
.....														

3 FITTING PROCEDURE FOR PEGASE

3.1 Theoretical SEDs of PEGASE

PEGASE is an evolutionary spectral synthesis model for starburst galaxies and normal galaxies of the Hubble sequence and is continuous over an exceptionally large wavelength range from 220 Å up to 50 000 Å. It is originally extended to the near-infrared (NIR) of the atlas of synthetic spectra of Rocca-Volmerange & Guiderdoni (1988) with a revised stellar library including cold star parameters and stellar tracks, which extended to the thermally-pulsing regime of the asymptotic giant branch and the post-AGB phase. The synthetic stellar spectral library is taken from Kurucz (1992), modified by Lejeune et al. (1997) to fit observed colors. A set of reference synthetic spectra at $z = 0$, to which the cosmological k- and evolution e-corrections for high-redshift galaxies are applied, is built from fits of observational templates (Fioc & Rocca-Volmerange 1997).

Assuming a standard IMF, SFR and other initial conditions, such as initial metallicity and extinction, we can compute the SED of galaxies at any stage of evolution within the metallicity range $Z = 0.0001 - 0.1$. Some factors, such as nebular emissions and dust effects are considered in the model. Typical prescriptions of PEGASE are the SFR and IMF.

The three forms of SFR, an instantaneous burst, a constant and an exponential rate with star formation scale $\tau = 1 - 15$ Gyr, are tested in this paper. Only the exponential form with $\tau = 3$ Gyr, (Exp ($\tau = 3$ Gyr)) is found to be satisfactory. The IMF is assumed to follow the Salpeter (1955) form, $\Phi(M) \propto M^{-\alpha}$ with $\alpha = 2.35$, with lower limit $M_{\rm l} = 0.1 M_{\odot}$, and upper limit $M_{\rm u} = 125 M_{\odot}$ (Sawicki & Yee 1998).

The initial parameters of the ESF used in PEGASE are given in Table 2.

3.2 Reddening Correction

Extinction affects the intrinsic colors of M81 and hence its accurate age estimation, so the photometric measurements must be de-reddened before the fitting procedure. The observed colors are in fact affected by two sources of reddening: (1) the foreground extinction in our Milky Way and (2) internal reddening due to the varying optical path through the disk of

M81. For the foreground extinction, Burstein & Heiles (1984) have measured a foreground color excess of 0.038 for M81, which we adopt here. In addition, we adopt the extinction curve presented by de Vaucouleurs et al. (1976). For the internal reddening of the galaxy, we take into account, in the PEGASE model, the extinction corresponding to a uniform plane-parallel slab at an inclination of 59°.

Table 2 Scenarios of Exponentially Decreasing Star Formation

IMF: Salpeter (1955)
Evolutionary tracks: "Padova"
Fraction of close binary systems: 0.05
Initial metallicity: 0.0
No infall
Type of star formation: exponentially decreasing
τ: 3.0 Gyr
Consistent evolution of the stellar metallicity
Mass fraction of substellar objects: 0.0
No galactic winds
Nebular emission
Extinction for a disk geometry
Specific Inclination: 59°

3.3 Flux Ratios of PEGASE

To determine the age distribution in M81 and its evolutionary history, we attempt to find the best match between observed colors and predictions of PEGASE for each of the cells of M81. Since the observational data include the integrated luminosity, to make a comparison, we first convolve the SEDs of PEGASE with the BATC filter transmission curve to obtain the integrated luminosity. The integrated luminosity of the ith BATC filter $L_{\lambda_i}(t)$ can be calculated by

$$L_{\lambda_i}(t) = \frac{\int F_\lambda(t)\varphi_i(\lambda)\mathrm{d}\lambda}{\int \varphi_i(\lambda)\mathrm{d}\lambda}\,, \tag{1}$$

where $F_\lambda(t)$ is the SED of PEGASE at age t, and $\varphi_i(\lambda)$ is the transmission curve of the i filter of the BATC filter system ($i = 2, 4, 5, ..., 15$).

For convenience, we follow Kong et al. (2000) and use flux ratios that are independent of distance. We calculate the flux ratio of the ith BATC filter relative to the 8th BATC filter ($\lambda = 6075\,\text{Å}$) (hereafter the flux ratio)

$$C_{\lambda_i}(t) = L_{\lambda_i}(t)/L_{6075}(t). \tag{2}$$

3.4 Fitting Algorithm

By minimizing the differences between a set of observed and synthetic SEDs, the best-fit evolutionary history of M81 can be found. The procedure is carried out by using:

$$\chi^2(x, y, t) = \frac{1}{d}\sum_{i=2,4}^{15}\left[\frac{C^{\mathrm{obs}}_{\lambda_i}(x, y) - C^{\mathrm{PE}}_{\lambda_i}(t)}{\sigma_{\lambda_i}}\right]^2, \tag{3}$$

where $C^{\mathrm{PE}}_{\lambda_i}(t)$ is the flux ratio in the ith filter of a PEGASE model at age t. $C^{\mathrm{obs}}_{\lambda_i}(x, y)$ represents the flux ratio for the cell at position (x, y), σ_{λ_i} is the uncertainty in the observed ith flux ratio, d is the number of degrees of freedom.

In this paper, the three forms of the SFR are considered. For the exponential form, SFR(t) $\propto \exp(-t/\tau)$, we examined, for values of $\tau = 1 - 15$ Gyr, the match between the observed and model-predicted colors. We find Exp ($\tau = 3$ Gyr) describes well the evolutionary history of M81.

Figure 1 compares the observed and the calculated best-fit flux ratios (as functions of the wavelength) for different cells of M81. It is clear that, for most of the cells, the exponential SFR gives the best fits among the three SFRs.

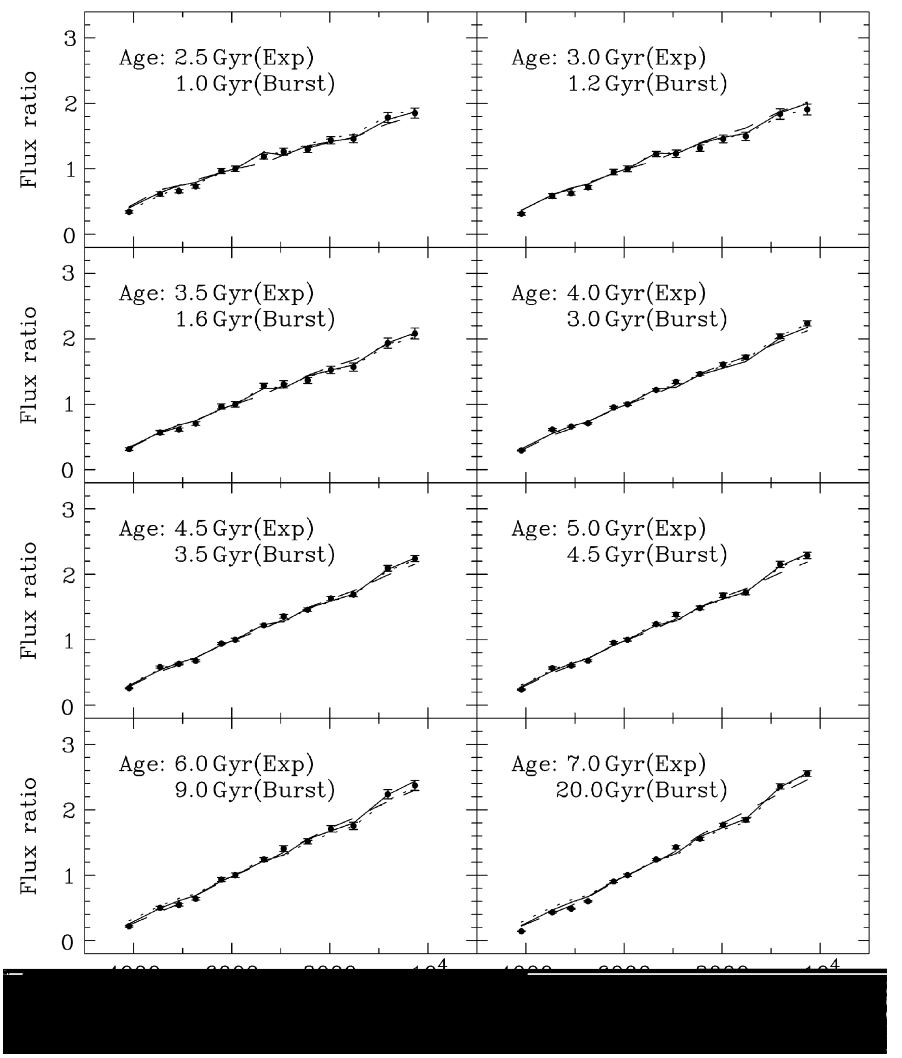

Fig. 1 Best PEGASE fits of the flux ratio profile for different cells of M81. Filled circles are the observed flux ratios. The PEGASE fits with the exponential, instantneous burst and constant SFR are shown by the solid, dashed, and dotted line, respectively.

4 AGE DISTRIBUTION AND EVOLUTIONARY HISTORY OF M81

Figure 2 presents the age histogram of M81 for the ESF model. The result shows that, in general, M81 has been forming stars continuously for the last 1–9 Gyr, with most stellar populations in the galaxy younger than 7 Gyr. The ages of the main components in the galaxy are from 3 Gyr to 6 Gyr.

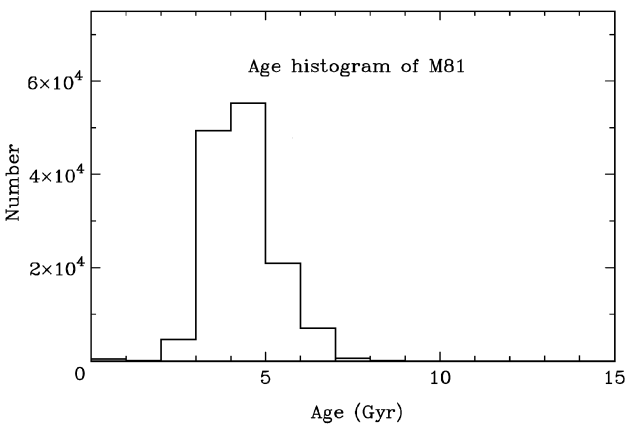

Fig. 2 Age histogram of M81 on ESF.

Figure 3 shows the map of age distribution of M81 on ESF. They are obtained by replacing the ADU of each pixel (cell) in the map with its corresponding fitting age. Light grey and dark grey represent the old and the young zones, respectively. For convenience, we shall call the innermost region inside the small polygon, the "central" zone; the region between the small

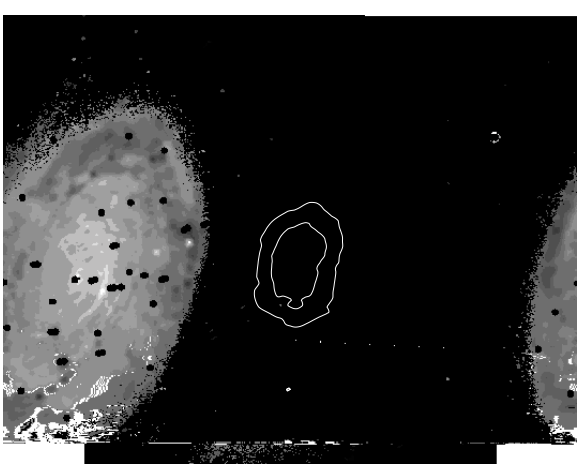

Fig. 3 Map of the age distribution of M81 based on ESF of PEGASE. Light gray corresponds to the old and dark gray to the young zones. Black spots represent the masked regions, such as most of the foreground stars, some HII regions and background galaxies.

and large polygon, the "bulge" area, and the region outside the large polygon, the "disk" region. The figure clearly shows that the components in the central zone are older than those in the outer regions. It also can be seen, though not quite so clearly, that the youngest components reside in places corresponding to the optical spiral arms. There is a clear age gradient from the center to the edge of the galaxy.

The ages in the central region and in some locations in the arc around it are greater than 8 Gyr. The age at the more extended region is about 7 Gyr. In the bulge edge area the age is about 6 Gyr. Stellar populations in the disk area are a little younger than those in the bulge region. The mean age in the disk area and its extension are about 4.5 and 3.5 Gyr, respectively. We can see that the age in the spiral arms is even less than in the inner areas, at about 2.5 Gyr.

5 DISCUSSION

5.1 Uncertainties

Galaxies are complex stellar systems containing populations of various ages and metallicities. It is difficult to separate the effects of age and metallicity. To isolate the effect of metallicity, Kong et al. (2000) obtained the metallicity distribution using the good correlation between the color index I_{8510} and the metallicity for BATC system by using GSSPs. Different from GSSPs, PEGASE can directly provide the stellar metallicity averaged on the bolometric luminosity. It can be shown (Figure 4) that there is a weak metallicity gradient from the central to the outer regions. Stellar populations in the bulge have the solar metallicity or higher; younger populations in the disk have metallicities lower than the sun. The range of the metallicity is from 0.016 to 0.022. As we know, the metallicity presented by PEGASE is the value averaged on the SSPs with various metallicities, and the average is sensitive to the dominant populations among all the SSPs. For PEGASE, at the present stage of evolution (corresponding to the observed SEDs), the dominant SSPs are those with metallicities between $Z = 0.02$ and $Z = 0.05$. Considering there are SSPs with metallicities lower than 0.02, it is reasonable to think that the mean metallicity is almost as same as the solar value.

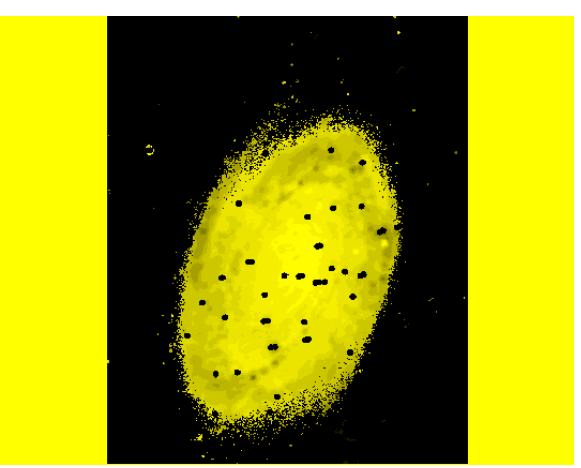

Fig. 4 Map of the metallicity distribution of M81. Light gray corresponds to high, and dark gray to low metallicity.

Besides the well-known age-metallicity degeneracy, there exists another effect, the effect of τ and t, which may significantly affect our attempts to derive an accurate reconstruction of the galaxy's star formation history. This also has been pointed out by Kong et al. (2000), although GSSPs was adopted there. For the exponential SFR, the effects of τ and t on the SEDs are different. True, in this case, the SFR depends only on the ratio t/τ, but if t is large, the SED of old red stars can result, which does not happen if t is small. Thus, if the error in the observed integrated luminosity is small enough, we can determine the values of τ and t simultaneously, at least we can limit the values of τ and t to within some small range. For an Sab spiral galaxy such as M81, the characteristic time scale of $\tau = 3$ Gyr obtained with our method is acceptable and is in agreement with the previous studies. For example, for Sa and Sb type spirals $\tau =$ 3 and 5 Gyr are respectively used in the Hyperz code (Bolzonella et al. 2000), and similar timescales are adopted in the Kennicutt model (Kennicutt 1983); Ann & Lee (1991) obtained τ values of 2.4 and 4.8 Gyr for Sa and Sb type galaxy using their photometric evolution model. After τ is fixed the age distribution follows.

5.2 Comparison with GSSPs

In their study on the structure of M81 with the BATC data, Kong et al. (2000) used GSSPs to derive the relative distributions of age, metallicity and reddening. They found that there is no obvious metallicity gradient from the central region to the bulge and disk, that the value of metallicity is likely to be within a range between $Z = 0.02$ and $Z = 0.05$, and that the mean metallicity is about 0.03, which is somewhat higher than our result. They also found a smooth age gradient from the center of the galaxy to the edge of the bulge. Their mean age of the stellar populations of each cell is greater than our result, except for the cells in the central regions. This can be seen in Table 3, which lists the age distributions of M81 on PEGASE by us and on GSSPs by Kong et al.

Now, the results obtained with GSSPs are based on the assumption that all the stars in a small region are coeval and share the same chemical composition, so that the stellar population of each cell can be modelled by one SSP. As we know, this ***strong*** assumption is appropriate for the description of simple systems such as globular clusters, but galaxies are complex systems formed with various stellar generations. So, as a simple model for describing the single burst of star formation, the GSSPs only provides an approximate indication of the relative ages of stellar populations. The original aim of Kong et al. (2000) was to check the variation of age and metallicity from the center to the edge of M81. If more information on the evolution of the galaxy is demanded, it would depend on a more complex evolutionary synthesis model. A major shortcoming of the GSSPs is that it omits the evolutionary history of the galaxy, but the history is important in the context of galaxy.

As an evolutionary synthesis model, PEGASE is modelled by integrating SSPs with the adopted star formation history and can give composite SEDs of various stellar generations. The advantage of PEGASE is that it directly describes the time evolution to, and after the present state (Fritze-v. Alvensleben 2000). The target of ESF is to present the evolutionary history and a more precise age distribution. This is the main reason why we use PEGASE. PEGASE has shortcomings too. Its basic shortcomings are due to fact that the evolutionary history of the galaxy is very complex and that some of the parameters in the model are degenerate, which may bring about uncertainties in the age estimates. Considering the complexity of the evolutionary history and the large number of possible adjustable parameters, we simply selected two, SFR and IMF, as adjustable, while adopting the default values in the PEGASE code for the other

input parameters.

In the fitting procedure it is found that for the bulge area the theoretical SEDs of PEGASE and GSSPs both give reasonable fits to the observed SEDs. This is because for the bulge area all the stellar populations are old and no young stars are forming. In this case, the stellar populations can be approximately regarded as SSPs so that there is almost no obvious difference between the SEDs of the two models. However, for the disk and star formation regions where stars are continuously forming young and old populations are mixed together. Thus, SSPs can be used to describe old populations of the bulge, but are not appropriate to describe the mixed stellar populations of the disk and the star formation regions. In fact, it can be found that in our fitting process ESF gives better fitting results than SSPs for most parts of the disk.

An SSP may be the simplest instantaneous burst model. We have compared the fitting results of GSSPs with that of the instantaneous burst of PEGASE. The age distribution is very similar, ranging from 1 to 15 Gyr, and the match between the synthesis and observed SEDs for GSSPs is a little better than that of the instantaneous burst.

Table 3 Comparison of Age Distributions of M81 for PEGASE and GSSPs

	Age (Gyr)		
Region	Exp ($\tau = 3$ Gyr)	starburst	GSSPs
innermost region	$\gtrsim 8$	$\gtrsim 15$	$\gtrsim 15$
central regions	7	8	9
bulge	6	4	4
disk	4.5	2	2
spiral arms	2.5	1.2	1

6 SUMMARY

Based on the large field multicolor observations of the BATC program, we study the structure, evolution and age distribution of M81 with an evolutionary synthesis code, PEGASE. Our main conclusions are summarised as follows.

1. With the help of PEGASE, we build different galaxy evolutionary models, according to the star formation at an instantaneous burst, or at a constant rate or at an exponential rate with star formation scale $\tau = 1 - 15$ Gyr. By fitting the flux ratios of each cell of M81 with the model predictions, we find the best fit is by the exponential SFR with $\tau = 3$ Gyr.

2. Comparing in detail the fitting results for each area obtained by PEGASE and GSSPs, we find that for most areas of M81, both codes give good matches between the synthesis and observed SEDs. Further analysis shows that the ESF of PEGASE is more appropriate for describing the evolution of M81.

3. From the age distribution of M81, we find that the mean ages of the stellar populations in the central regions are greater than those in the outer regions. This suggests that star formation in the central regions occurred earlier than in the outer regions; the formation of the stellar populations in the spiral arms is the most recent, indicating that a large number of stars are even now forming there. It can also be shown that star formation in M81 has occurred almost continuously for $1 - 9$ Gyr, and that most of the observed stellar populations in it are younger than 7 Gyr.

4. From the two-dimensional metallicity map of M81, we find a weak metallicity gradient from the central regions to the outer regions. The range of the metallicity is from 0.016 to 0.022.

Acknowledgements We are indebted to an anonymous referee for critical and helpful comments that improved the paper. We would like to thank Professor Zhen-Long Zou, Dr. Hong Wu, Yan-Bin Yang, Xian-Zhong Zheng, especially Xu Kong and Michel Fioc for fruitful discussions. We also appreciate the assistants who contributed their hard work to the observations. This work was funded by the National Key Base Sciences Research Foundation (NKBRSF, TG199075402) and is also supported by the National Natural Science Foundation of China (No. 10273012).

References

Ann H. B., Lee C. W., 1991, JKAS, 24, 13
Bolzonella M., Miralles J. M., Pelló R., 2000, A&A, 363, 476
Bruzual G., Charlot S., 1993, ApJ, 405, 538
Bruzual G., Charlot S., 1996, Documentation for GISSEL96 Spectral Synthesis Code
Burstein D., Heiles C., 1984, ApJS, 54, 33
Buzzoni A., 1999, In: IAU Symp. 183, Cosmological Parameters and the Evolution of the Universe, ed. K. Sato, 18
Charlot S., Bruzual G., 1991, ApJ, 367, 126
de Vaucouleurs G., de Vaucouleurs A., Corwin H., 1976, Second Reference Catalogue of Bright Galaxies, Austin: Univ. Texas Press
Fan X. H., Burstein D., Chen J. S. et al., 1996, AJ, 112, 628
Fioc M., Rocca-Volmerange B., 1997, A&A, 326, 950
Freedman W. L., Hughes S. M., Madore B. F. et al., 1994, ApJ, 427, 628
Fritze-v. Alvensleben U., 2000, ASP Conf. Ser. 221, Stars, Gas and Dust in Galaxies: Exploring the Links, 179
Guidedoni B., Rocca-Volmerange B., 1987, A&A, 186, 1
Heckman T. M., Balick B., Crane P. C., 1980, A&AS, 40, 295
Jacoby G. H., Ciardullo R., Ford H. C., Booth J., 1989, ApJ, 344, 704
Kennicutt R. C., 1983, ApJ, 272, 54
Kewley L. J., Dopita M. A., Sutherland R. S., Heisler C. A., Trevena J., 2001, ApJ, 556, 121
Kong X., Zhou X., Cheng J. S. et al., 2000, AJ, 119, 2745
Kurucz R. L., 1992, Model Atmospheres for Population Synthesis, ed. Barbuy B., Renzini A., The stellar population of Galaxies, IAU Symp. 149, Reidel: Dordrecht, 225
Leitherer C., Schaerer D., Goldader J. D. et al., 1999, ApJS, 123, 3
Lejeune Th., Cuisinier F., Buser R., 1997, A&AS, 125, 229
Peimbert M., Torres-Peimbert S., 1981, ApJ, 245, 845
Rocca-Volmerange B., Guiderdoni B., 1988, A&AS, 75, 93
Salpeter E. E., 1955, ApJ, 121, 161
Sawicki M., Yee H. K. C., 1998, AJ, 115, 1329
Searle L., Sargent W. L. W., Bagnuolo W. G., 1973, ApJ, 179, 427
Tinsley B. M., 1972, A&A, 20, 383
Zheng Z. Y., Shang Z. H., Su H. J. et al., 1999, AJ, 117, 2757
Zhou X., Chen J. S., Zhu J. et al., 2001, Chin. J. Astron. Astrophys., 1, 372
Zhou X., Jiang Z. J., Ma J. et al., 2003, A&A, 397, 361